Journal of Theoretical and Applied Information Technology
15th April 2018. Vol.96. No 7

ISSN: 1992-8645 www.jatit.org E-ISSN: 1817-3195

A NEW TECHNIQUE FOR ESTIMATING AND ENHANCING ORIENTATION FIELD OF FINGERPRINT IMAGE

ALAA AHMED ABBOOD[1*], GHAZALI SULONG[2], AHMED MAJID TAHA [3,4]
SABINE U.PETERS[5]

[1] Faculty of Business Informatics, University Of Information Technology and Communications (UOITC), Baghdad, Iraq
aaalaa2@uoitc.edu.iq
[2]UTM-IRDA Digital Media Centre (MaGIC-X), Faculty of Computing, University Technology Malaysia, 81310Skudai, Johor Bahru, Malaysia
ghazali@spaceutm.edu.my
[3]Faculty of Business Informatics, University Of Information Technology and Communications (UOITC), Baghdad, Iraq
[4] Soft Computing and Data Mining Center, Universiti Tun Hussein Onn Malaysia 86400 Parit Raja, Batu Pahat Johor, Malaysia
E-mail: ahmed.majid.taha@gmail.com.

[5]College of Education, Florida State University, Tallahassee, 32306 Florida, USA
supeters67@gmail.com

ABSTRACT

The direction of fingerprint patterns normally changes from one block to another, which makes it necessary to have information about neighbouring blocks to obtain the original shape of the fingerprint patterns. This paper introduced a novel approach for orientation field calculation using an innovative filter formed as Epicycloid window shape. In which estimates the orientation fields of each block in the main space of work, to create true-angle orientation fields. The calculation procedure of the proposed method is executed by first dividing the image into blocks of pixels with size (16x16). Then, Epicycloid shape filter with $\boldsymbol{k = 4}$ is located surrounding the target block to extract some information from its **8** neighbours. Finally, calculate the local gradient for each target block which is values later used to estimate the gradient angle $\boldsymbol{\theta}$ for that block. The obtained patterns then grouped together to form four distinct homogenous regions using a region growing technique. The current method was evaluated using the NIST-14 database and showed reliable results on different quality images.

Keywords: *Fingerprint Image Enhancement, Orientation Field Estimations, Epicycloid Window Shape Filter, Region-Growing Technique, Feature Extraction*

1. INTRODUCTION

Biometrics are measurable characteristics based on physiological and behavioural traits that are used in the identification of individuals. The most important type of human biometrics is a fingerprint. Fingerprints have been used for personal recognition in forensic applications such as criminal investigation tools and in civilian applications, as well as border access control systems, national identity card validation and authentication processors. The uniqueness and immutability of fingerprint patterns as well as the low cost of associated biometric equipment make fingerprints more desirable than the other types of biometrics [1][2]. An automatic fingerprint recognition system (AFIS) often includes the some processes such as: fingerprint acquisition; image pre-processing (fingerprint segmentation, enhancement and the orientation field estimation), fingerprint classification, minutiae detection and matching [3].

The process of estimating the local ridge direction of fingerprint images is referred to as orientation field estimation. Fingerprint images are often viewed as oriented textures by assuming a local ridge flow. The accuracy of fingerprint orientation field estimation is the most important step in detecting a singular point, and with that ensuring a high level of accuracy of a fingerprint classification system [4]. However, false

Journal of Theoretical and Applied Information Technology
15th April 2018. Vol.96. No 7

ISSN: 1992-8645 www.jatit.org E-ISSN: 1817-3195

orientations are inevitable because of distortions due to impressions and skin conditions. Low-quality regions pose a great threat to both feature extraction and fingerprint classification, since their positions and sizes are unpredictable, which make their effect on fingerprint processing systems unpredictable, as well. Therefore, it is very important to improve a fingerprint image's orientation field accuracy, thus facilitating image feature extraction for fingerprint classification [5] .

The research focused on the FE orientation field estimation techniques that have been considered for fingerprint classification, leaving, for the sake of brevity, out of the scope of this work those models developed for other purposes in fingerprint identification. However, this is in fact one of the issues that new fingerprint classification developments should take into account. There are many preprocessing algorithms for fingerprint enhancement which has many effect on the performance of fingerprint identification system. Most of these techniques provide ways of obtaining more accurate features that should serve new FE methods being more robust against the quality of the fingerprints [6].

A fingerprint expert can identify fingerprint ridges and valleys using various clues including local ridge orientation, ridge continuity and ridge tendency. Fingerprints tend to have varying flow directions with some singularities. As long as a print's ridge and valley structures are not corrupted completely, it is possible to develop an algorithm to improve orientation estimation accuracy and increase the efficiency and the robustness of fingerprint processing systems. Therefore, the challenge is to accommodate the unpredictability of unreliable regions using existing image information while still preserving the actual ridge flow.

2. RELATED WORK

Over the years, many methods like the gradient method, polynomial model method, normal vector method, gabor filter-bank method, multi-scale directional operator method, and line sensor method have been applied to estimate the orientation field of fingerprint patterns [2][7][8][9][10]. Zhu et al., (2006) implemented the neural network method to design a systematic scheme to estimate fingerprint ridge orientations. Here, the estimated ridge orientation was obtained by evaluating the correctness of ridge orientations. The purpose for this neural network was to determine the correctness of the estimated orientation used in the gradient-based approach.

The gradient approach has been widely used for estimating local ridge directions and that is based on the computation of fingerprint image gradients. This method facilitates the calculation of orientation fields of non-overlapping pixel blocks by examining the gradients of pixel intensities in the $\boldsymbol{x}$ and $\boldsymbol{y}$ directions within a given block.

For a given fingerprint image, the ridge flow direction at every pixel (i,j) consists of an angle $\theta_{xy}(i,j)$ that indicates the direction of flow with respect to the horizontal axis (see Figure 1). The value of $\theta_{xy}(i,j)$ can be uniquely determined only in $[0,\pi]$ if the opposite ridge flow directions are equivalent.

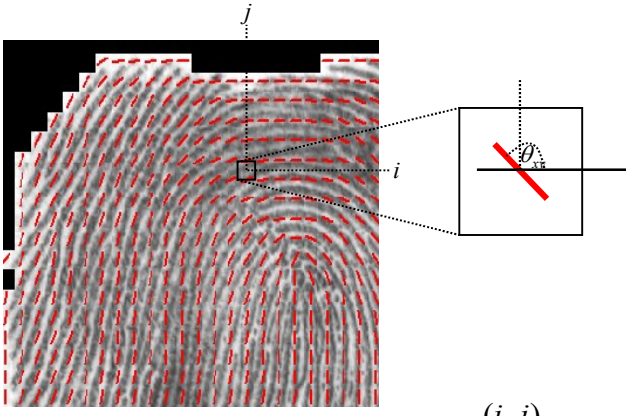

Figure 1 Ridge flow direction at pixel (i,j) and angle $\theta_{xy}(i,j)$ indicating the direction of flow with respect to the horizontal axis

The gradient is two-dimensionally equivalent to the first derivative and is defined as vector (1):

$$G\left[F_{xy}(i,j)\right] = \begin{bmatrix} G_x(i,j) \\ G_y(i,j) \end{bmatrix} \quad (1)$$

Where $G_x(i,j) = \frac{\partial f}{\partial x}$ and $G_y(i,j) = \frac{\partial f}{\partial y}$ components are the derivatives of F in $[x_i, y_i]$ with respect to the x and y directions in the Cartesian system. The gradient phase angle denotes the direction of the maximum pixel-intensity change, and the magnitude of the gradient is defined as the square root of the number of gradient directions x and y. Gradient component derivatives $G_x(i,j)$ and $G_y(i,j)$ are approximated through many operators, most commonly the Sobel operator. The Sobel

ISSN: 1992-8645 www.jatit.org E-ISSN: 1817-3195

operator uses a 3×3 neighbourhood for the gradient, as shown in Equation (2) below.

$$G_x = \begin{bmatrix} 1 & 0 & -1 \\ 2 & 0 & -2 \\ 1 & 0 & -1 \end{bmatrix}, \quad G_y \begin{bmatrix} 1 & 2 & 1 \\ 0 & 0 & 0 \\ -1 & -2 & -1 \end{bmatrix} \quad (2)$$

The Sobel method, though easy to use and very efficient, presents some challenges with regards to its nonlinearity and discontinuity. For instance, using the Sobel operator to estimate component $G_x(i,j)$, $G_y(i,j)$and computing $\theta_{xy}(i,j)$ as the arctangent of the $G_y(i,j)/\ G_x(i,j)$ ratio, produces a non-linear output and also causes discontinuity at around 90 of image gradient direction. On the other hand, if a single orientation estimate that describes the ridge-valley direction is measured using an extremely scale, the observed measurement value generally becomes very sensitive to noise. Witkin (1987) developed an approach to reduce nonlinearity and discontinuity by doubling the gradient direction angles [11]. He found that by doubling the angles and squaring the length of the gradient, the gradient vector can be converted to a polar system. This approach assumes $G_x(i,j) = r\cos\theta_{xy}(i,j)$ and $G_y(i,j) = r\sin\theta_{xy}(i,j)$ where $-\frac{1}{2}\pi < \theta_{xy} \leq \frac{1}{2}\pi$. A 2D equivalent of the first gradient derivative is defined as the vector using Equation (3):

$$G[F_{xy}(i,j)] = \begin{bmatrix} r\sin 2\theta_{xy}(i,j) \\ r\cos 2\theta_{xy}(i,j) \end{bmatrix} \quad (3)$$

However, Ratha *et al.* (1995) obtained a dominant direction using 16x16 block, which is given as (4):

$$\theta_d = \frac{1}{2}\, tan^{-1}\left(\frac{\sum_{i=1}^{16}\sum_{j=1}^{16} 2G_x(i,j)G_y(i,j)}{\sum_{i=1}^{16}\sum_{j=1}^{16}(G_x(i,j)^2 - G_y(i,j)^2)}\right) \quad (4)$$

Where $G_x(i,j) \neq 0$ and $G_y(i,j) \neq 0$ the angle θ_d is only quantized into 16 directions.

[8] also utilized principal component analysis (PCA) for estimating fingerprint image orientation fields and extracted local ridge orientations by averaging squared gradients. The average of squared gradient direction is given as $\theta_{xy}(i,j)$, with $-\frac{1}{2}\pi < \theta_{xy}(i,j) \leq \frac{1}{2}\pi$.

The gradient-based approach is popular among researchers for calculating the orientation field in fingerprint images. This can be accomplished by taking the partial derivatives of grey values at every pixel, and then calculating the orientation by averaging the squared gradient in a restricted neighbours [12]. The gradient-based approach makes estimating the local ridge orientation efficient and accurate. However, this process is also sensitive to image noise such as dirt, wetness, wrinkles and cuts. Reconstruction methods like low-pass filters have been applied to improve the smoothing of the orientation field estimation in corrupted areas [13].

Typically, the calculation of the orientation field estimation is based on $w \times w$ non-overlapping block of pixels and a single local ridge orientation is defined for each block. Researchers have traditionally used non-overlapping blocks, but there are no standard block sizes. Commonly used block sizes mentioned in many literature are 8×8, 16×16 or 32×32 pixels, which means that the block size depends on the experiments carried out by the authors[14][14][14][14][14] [6].Increasing the size of the block typically results in decreased sensitivity to noise but also produces inaccurate estimation of the actual shape structure of fingerprint patterns. Reducing the block size improves estimation accuracy but amplifies the sensitivity to image noise.

Another orientation field estimation technique was found in the research of Sherlock., (1993) were suggested implementing fingerprint orientation field estimation from Core and Delta positions [11]. This approach uses a zero-pole model which sets the Core point at 0 and the Delta point as a pole and frequently results in the correct detection of singular points, bringing about an accurate orientation field estimation [11], [15]. The drawback of this method is that it does not cover the same shape structure of the orientation field estimation, and it may not detect a singular point at the same location when fingerprints have different ridge patterns. According to Vizcaya and Gerhardt (1996), this approach can be improved by using a piece-wise linear approximation around the singular points to adjust zero and pole behaviours. Unfortunately, zero-pole models depend on

ISSN: 1992-8645 www.jatit.org E-ISSN: 1817-3195

singular point positions. Hence, this model may not work well with fingerprint images that have no singular points or only one type of singular points [16].

[10] proposed an algorithm for modelling the fingerprint orientation field estimation by reconstructs the orientation using data from around singular points. This algorithm consists of two steps. For the first step, an orientation prediction is made based on a piece-wise first order phase portrait model. The initial estimation of an orientation field is calculated using a gradient-based approach to increase the orientation prediction accuracy. For the second step, a constrained nonlinear phase portrait algorithm is applied to obtain the final orientation model [17], [18].

Fingerprint ridge orientation can be estimated by evaluating the correctness of ridge orientation fields using machine learning in neural network configurations [6], [9]. Improvements in the estimation of fingerprint ridge orientations were proposed by Ji and Yi (2008) who used four-direction orientation fields. Ji and Yi's method consists of four steps. In the first step, the fingerprint is segmented and binarized. During the second step, the primary ridge of the fingerprint block is determined using neuron pulses coupled with a neural network. In the third step, the block direction is estimated by defining four discrete directions to represent a fingerprint orientation field. Finally, the estimation field is corrected by comparing the ridges and valleys of the original orientation estimation [19], [20].

In this study, a new method for orientation field calculation using an innovative filter, which is based on Epicycloid window shape, is introduced. Details are discussed in the next section.

3. METHODOLGY

3.1 Fingerprint pre-processes

3.1.1 Fingerprint Image Enhancement

In order to develop a high performance Automatic Fingerprint Identification System, image quality is a key factor. Fingerprint image samples are often distorted by smudges or blotches. In poor quality fingerprint images, the valleys and ridges are not clear and discontinuities exist in the ridges and are often caused by random interference in the capturing devices [6]. Overcoming the problems related to extreme contrast conditions (low contrast or high contrast) and associated discontinuities of the fingerprint patterns is a challenge. Therefore, it is necessary to apply fingerprint image enhancement before any classification procedure [21]. In this study, fingerprint images were normalized by using grayscale normalization to standardize the intensity of the pixels, and the contrast of the images were improved using Histogram Equalization. To solve the problem of discontinuity, Binarization and Skeletonization approaches were applied. In the final step, Fusion algorithms were applied to the output image, and with the help of Skeletonization and Histogram Equalization, enhanced the quality of fingerprint images as in the Figure 2 below.

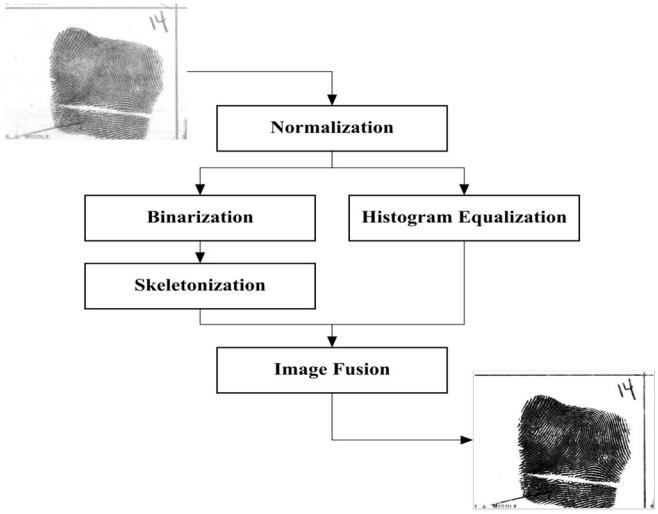

Figure 2 The proposed enhanced fingerprint image technique

3.1.2 Proposed Segmentation Technique

Fingerprint Segmentation isolates features that have similar characteristics. During this process, the fingerprint image is split into foreground and background regions. The foreground region contains fingerprint image information about ridges and valleys, while the background region represents fingerprint image borders. Image quality is vital for segmentation to be accurate, so the input image of the segmentation process is actually the output image from the enhancement process. This segmentation process generally depends on threshold values that differ from one block to another based on the grey-level

ISSN: 1992-8645 www.jatit.org E-ISSN: 1817-3195

of images. In this study, new segmentation method is proposed based on automatic threshold values [11]. The three essential steps implemented in this current segmentation method include a statistical calculation of the fingerprint image features to obtain the threshold values.

Before the segmentation process could begin, the optimal threshold value was determined using statistical calculations based on the three parameters mean, variance and gradient coherence. The global mean represents the arithmetic average of the intensity values of the image and was calculated using the equation in (5). The local mean $M_b(i,j)$ represents the arithmetic average of the intensity values of the block size $w \times w$ and calculated using equation (6).

$$M_b(i,j) = \frac{1}{w \times w} \sum_{u=i}^{i+w-1} \sum_{v=j}^{j+w-1} I(u,v) \qquad (5)$$

The local variance $V_b(i,j)$ represents the arithmetic average of the squared differences between the intensity values and the local mean, see equation (6).

$$V_b(i,j) = \frac{1}{w \times w} \sum_{u=i}^{i+W-1} \sum_{v=j}^{j+w-1} (I(u,v) - M_b(i,j))^2 \qquad (6)$$

Where $I(u,v)$ represents $(u,v)^{th}$ block of image I, and $w = 16$.

The gradient coherence feature indicates the strength of the local window gradients centred on the processed point along the same dominant orientation. The gradient coherence parameter is used here to describe the variation of grey-level values in the fingerprint images. The gradient coherence $coh(i,j)$ for the block size $w \times w$ is calculated as shown in (7):

$$coh(i,j) = \frac{\sqrt{(g_x(i,j) - g_y(i,j)) + 4(g_{xy}(i,j))^2}}{(g_x(i,j) + g_y(i,j))} \qquad (7)$$

Where

$$g_x(i,j) = \sum_{u=i}^{i+w-1} \sum_{v=j}^{j+w-1} BG_x(u,v)^2 \qquad (8)$$

$$g_y(i,j) = \sum_{u=i}^{i+w-1} \sum_{v=j}^{j+w-1} BG_y(u,v)^2 \qquad (9)$$

$$g_{xy}(i,j) = \sum_{u=i}^{i+w-1} \sum_{v=j}^{j+w-1} BG_x(u,v)\ BG_x(u,v) \qquad (10)$$

Where $BG_x(u,v)$ and $BG_y(u,v)$ are corresponding horizontal and vertical basic gradient components at (u,v) and calculated as follows:

$$BG_x(u,v) = \sum_{m=-1}^{1} \sum_{n=-1}^{1} (S_x(m,n) \times I(u+m, v+n)) \qquad (11)$$

$$BG_y(u,v) = \sum_{m=-1}^{1} \sum_{n=-1}^{1} (S_y(m,n) \times I(u+m, v+n)) \qquad (12)$$

Where $(S_x(m,n))$ is the Horizontal Sobel mask operator, and $(S_y(m,n))$ is the Vertical Sobel mask operator, as shown in (13)

$$S_x = \begin{bmatrix} 1 & 0 & -1 \\ 2 & 0 & -2 \\ 1 & 0 & -1 \end{bmatrix}, \quad S_y = \begin{bmatrix} 1 & 2 & 1 \\ 0 & 0 & 0 \\ -1 & -2 & -1 \end{bmatrix} \qquad (13)$$

3.2 Proposed Orientation Field Estimation using Epicycloid Windows Shape

In geometry, an epicycloid is a plane curve produced by tracing the path of a chosen point of a ***k*** circle which rolls without slipping around a fixed point. Figure 3 shows some examples of Epicycloid shapes with a different k value (Lawrence J. D., (2013).

Journal of Theoretical and Applied Information Technology
15th April 2018. Vol.96. No 7

ISSN: 1992-8645 www.jatit.org E-ISSN: 1817-3195

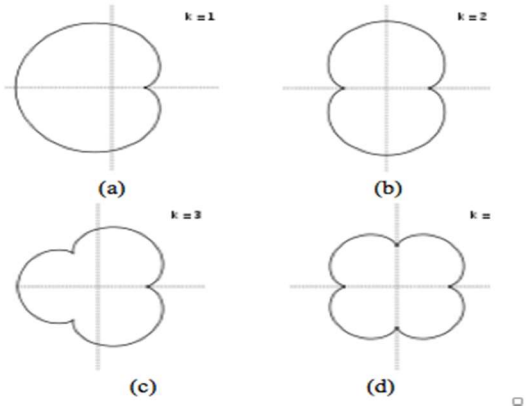

Figure 3: Epicycloid shapes with (a) $k = 1$, (b) $k = 2$, (c) $k = 3$ and, (d) $k = 4$ (Lawrence, 2013)

In this study, Epicycloid shape with $k = 4$ (refer to Figure 4) is used to estimate the orientation field of fingerprint patterns, because this shape covered sufficient information about the neighbour blocks. The calculation procedure of this method depends on individual block positions and is executed by first dividing the image into blocks of pixels, and Epicycloid shape with $k = 4$ is located surrounding the target block to extract some information from its 8 neighbours.

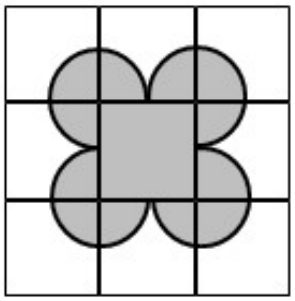

Figure 4: Epicycloid window shape over 3x3 blocks

The calculation of orientation fields is performed by introducing a new filter or mask of size 3 x 3 blocks (where each block has 16×16 pixels), which utilizes the above Epicycloid shape. Hereinafter, the filter is called Epicycloid Filter or EF in short. The elements of this filter are set as 1 for all pixels inside the Epicycloid shape and 0 for the pixels outside this shape as in Figure 5 bellow.

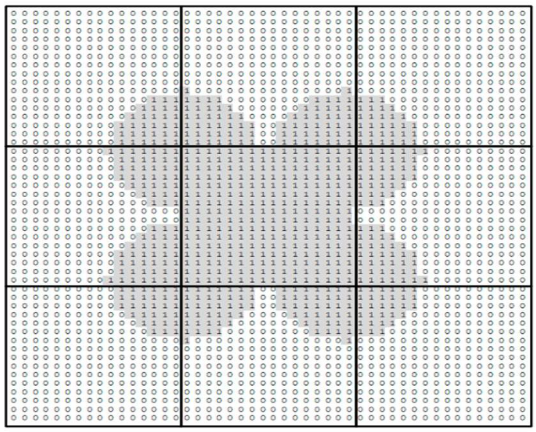

Figure 5: The Epicycloid Filter (EF)

The processes of orientation field calculation are summarized as follows:

Compute the gradients $G_x(u,v)$ and $G_y(u,v)$ for each pixel of $I(u,v)$ image using Sobel operator as in equations (14) and (15) respectively.

$$G_x(u,v) = \begin{bmatrix} 1 & 0 & -1 \\ 2 & 0 & -2 \\ 1 & 0 & -1 \end{bmatrix} \times \begin{bmatrix} u-1,v-1 & u,v-1 & u+1,v-1 \\ u-1,v & u,v & u+1,v \\ u-1,v+1 & u,v+1 & u+1,v+1 \end{bmatrix} \quad (14)$$

$$G_y(u,v) = \begin{bmatrix} 1 & 2 & 1 \\ 0 & 0 & 0 \\ -1 & -2 & -1 \end{bmatrix} \times \begin{bmatrix} u-1,v-1 & u,v-1 & u+1,v-1 \\ u-1,v & u,v & u+1,v \\ u-1,v+1 & u,v+1 & u+1,v+1 \end{bmatrix} \quad (15)$$

Divide $\boldsymbol{I(u,v)}$ image into blocks of 16×16 pixels.

Scan the image from the top-left corner to the right-bottom corner using the EF, one target block at a time (refer to Figure 4), and then calculate the local gradient $V_x(i,j)$ and $V_y(i,j)$ for each target block (i,j) using equations (16) and (17) as below:

$$\mathbf{V_x(i,j)} = \sum_{u=-16}^{31} \sum_{v=-16}^{31} \begin{pmatrix} \mathbf{2\, G_x(16 \times i + u - 16, 16 \times j + v - 16)} \\ \mathbf{G_y(16 \times i + u - 16, 16 \times j + v - 16)} \end{pmatrix} * \mathbf{M(u+16, v+16)} \quad (16)$$

$$\mathbf{V_y(i,j)} = \sum_{u=-16}^{31} \sum_{v=-16}^{31} (\mathbf{G_x^2(16 \times i + u - 16, 16 \times j + v - 16) - G_y^2(16 \times i + u - 16, 16 \times j + v - 16))} * \mathbf{M(u+16, v+16)} \quad (17)$$

Where M represents the EF given in the Figure 6.

Journal of Theoretical and Applied Information Technology
15th April 2018. Vol.96. No 7

ISSN: 1992-8645 www.jatit.org E-ISSN: 1817-3195

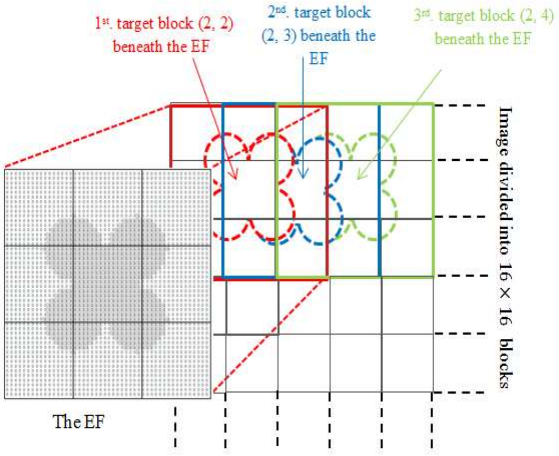

Figure 6: Blocks beneath the mask

For a given fingerprint image, the ridge flow direction at every pixel (i,j) consists of an angle $\theta_{xy}(i,j)$ that indicates the direction of flow with respect to the horizontal axis. The value of $\theta_{xy}(i,j)$ can be uniquely determined only in $[0,\pi]$ if the opposite ridge flow directions are equivalent. Therefore, the calculation of the gradient angle $\theta(i,j)$ for each target block is done using equation (18).

$$\theta(i,j) = \frac{1}{2}\arctan\left(\frac{V_x(i,j)}{V_y(i,j)}\right) \qquad (18)$$

The values of θ(i,j) are between −90° to +90°, but in the fingerprint the required values of θ(i,j) must be between 0° to 180°, so the values of θ(i,j) are normalized using equation (19).

$$\theta'(i,j) = \begin{cases} \theta(i,j) & if\ V_x(i,j) > 0\ and\ V_y(i,j) \geq 0 \\ \theta(i,j) + \pi & if\ V_x(i,j) < 0\ and\ V_y(i,j) \geq 0 \\ \theta(i,j) + \frac{\pi}{2} & if\ V_x(i,j) < 0\ and\ V_y(i,j) \leq 0 \\ \theta(i,j) + \frac{\pi}{2} & if\ V_x(i,j) > 0\ and\ V_y(i,j) \leq 0 \end{cases} \qquad (19)$$

(10)

An example of a fingerprint image that has gone through the orientation field estimation process is provided in Figure 7.

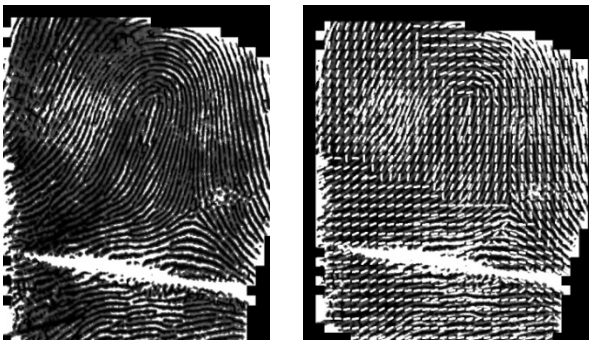

(a) (b)

Figure : The orientation field process: (a) Segmented fingerprint image (b) Orientation fingerprint image

3.3 Highlighting the Homogeneous Area in Fingerprint Image based on Region Growing Technique (RGT).

Upon completion of the orientation fields angle $\theta(i,j)$ calculation, following process is to divide the foreground into four exclusive homogenous regions in terms of the angle θ, according to the following four intervals: $0^\circ - 45^\circ$, $45^\circ - 90^\circ$, $90^\circ - 135^\circ$ and $135^\circ - 180^\circ$. To come out with a perfect, clean and unstained homogenous region is challenging. Previously, homogenous area detection used by earlier researchers was based on user pre-defined colours for certain range of angles, and this was found to have high sensitive to noise caused by non-uniform distribution of pixels intensity in the homogeneous area [22]. Due to that, some parts of the homogenous areas are stained. Thus, this study introduces a new method based on region growing technique to detect the homogeneous areas in the fingerprint image, and is summarized as follow:

1. Set all the image blocks as unlabelled.
2. Select a set of blocks as seeds. Theses seeds are determined by separating range of angles θ into 15° increments. These blocks are then labelled by colour into four groups. Green from 15° to 30°, red from 60° to 75°, purple from 105° to 120° and blue from 150° to 165°, as shown in Figure 8. The initial region begins from the location of these seeds.

Journal of Theoretical and Applied Information Technology
15th April 2018. Vol.96. No 7

ISSN: 1992-8645 www.jatit.org E-ISSN: 1817-3195

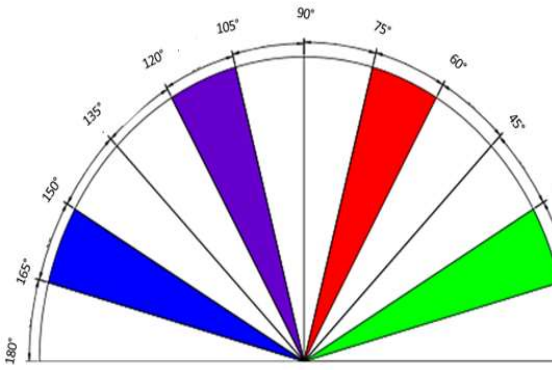

Figure 8: Seed label according to colour

3. Calculate the difference in angles θ between each seed block and their surrounding neighbours. The blocks in which the difference with the seed block is minimal, take the same colour of the seed block. These blocks in their turn became seed blocks as shown in Figure 9 (a) to (c).

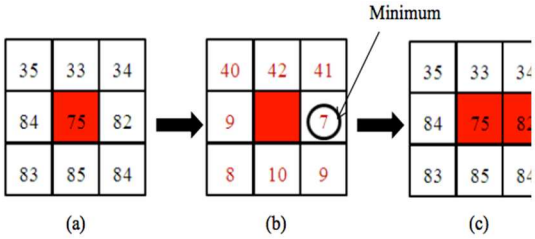

Figure 9: Process of growing for one seed (a) Seed block with its surrounding neighbours (b) Difference in values to seed block (c) Spreading of the colour.

4. The region stops growing when all blocks were labelled and satisfied the homogeneity criterion.

Algorithm 1: Shows The Processes of Homogenous Area Detection Using Region Growing Technique

```
Input: Orientation Field Image of size H H H .
Output: Homogenous regions HR.
  Begin:
    for i= 1 → W, increment by 16 do
      for j= 1 → H, increment by 16 do
        If θ( i ,j) = 15 && θ( i ,j) = 30
          HR ( i ,j) ← 'G';
        end If
        If θ( i ,j) = 60 && θ( i ,j) = 75
          HR ( i ,j) ← 'R';
        end If
        If θ( i ,j) = 105 && θ( i ,j) = 120
          HR ( i ,j) ← 'P';
        end If
        If θ( i ,j) = 150 && θ( i ,j) = 165
          HR ( i ,j) ← 'B';
        end If
      end for
    end for

    for i= 1 → W, increment by 16 do
      for j= 1 → H, increment by 16 do
        If HR( i ,j) not Classified
          Min ← +H;
          for u= -1 → 1, increment by 1 do
            for v= -1 → 1, increment by 1 do
              d ← (|θ( i ,j)-θ(i+u ,j+v)|+180)% 180
              If d < Min
                Min ← d;
                HR( i ,j) ← HR ( i+u ,j+v);
              end If
            end for
          end for
        end If
      end for
    end for
  End
```

As earlier mentioned the fingerprint image is divided into four homogenous regions, these regions are labelled using the colours, green, red, purple and blue. The process of achieving the regions is illustrated in the Figure 8 (a), (b), though the detailed explanation of how the regions are grown has earlier been presented using an instance of RGT.

An example of a fingerprint image that has gone through the Region Growing Technique is provided in Figure 10.

Journal of Theoretical and Applied Information Technology
15th April 2018. Vol.96. No 7

ISSN: 1992-8645 www.jatit.org E-ISSN: 1817-3195

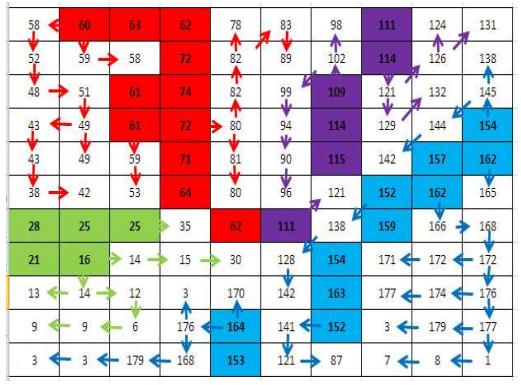

(a)

(b)

Figure 10(a) The distribution of the seed points for region growing in an image (b) The resultant labelled blocks formed from (a).

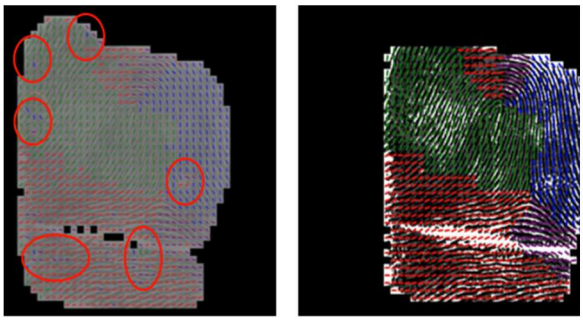

(a) (b)

Figure 11 (a) Fingerprint image with 4 homogenous regions detected using existing method used by [13] (b) Fingerprint image with 4 homogenous regions detected using RGT method

The details of all the above processes are summarized in the Figure (12) bellow:

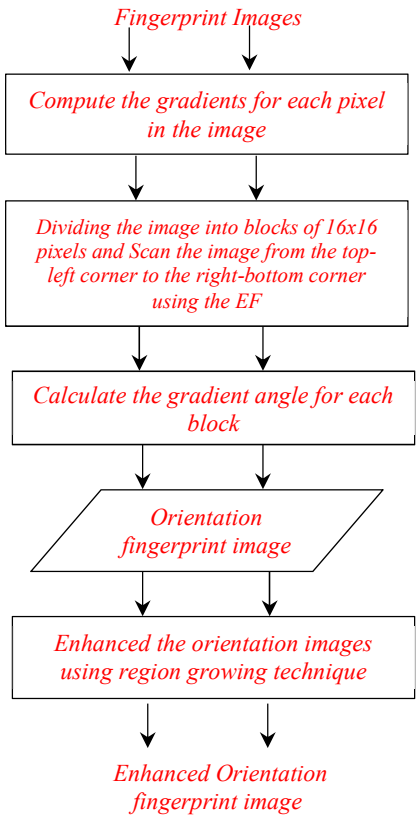

Figure 12 summary of all the processes used in current method

4. RESULT AND DISCUSSIONS

The capturing of ridge structures in fingerprint images is done by means of an orientation field estimation process. This process is considered an essential step because the reliability of singular points is highly depended on the accuracy of this process. In this study, two techniques were combined to obtain enhanced orientation field images: The current Fingerprint Epicycloid filter that is designed to estimate the fingerprint patterns, and the Region Growing technique that detects the homogenous regions of the fingerprint images. In order to conduct a comprehensive evaluation of the effectiveness of this orientation field estimation process, images of various qualities, such as good, dry, low-contrast and wet were used in this study.

The differences between the two methods using good quality images were not immediately apparent. However, the existing methods resulted in parts of homogenous regions tainted with alien

Journal of Theoretical and Applied Information Technology
15th April 2018. Vol.96. No 7

ISSN: 1992-8645 www.jatit.org E-ISSN: 1817-3195

colours, while the current method did not. The effectiveness of the current method may be attributed to the Region Growing technique, which has highlighted these patterns accurately. Figure 13 bellow shows a visual representation of the difference between the current and existing approaches on good quality images

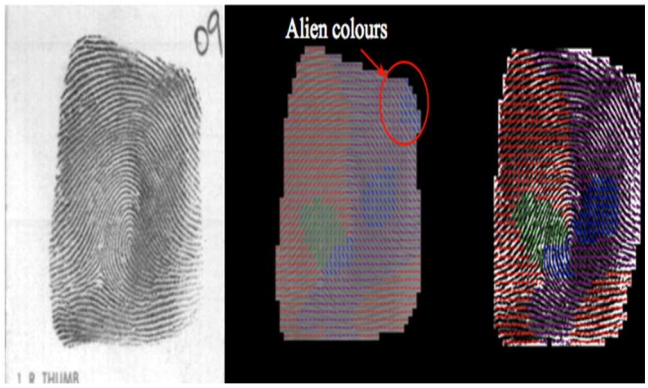

Figure 13: Orientation fields of good quality images: Current method versus existing method.

Based on visual inspections, the current method shows a significant improvement in the ability to estimate fingerprint patterns of different quality images. This may be attributed to two factors: (1) the current method calculated the orientation field of each block based on its pixels' gradient values as well as the gradient values of its neighbouring blocks' pixels using the FE filter; and (2) the Region Growing process corrected any erroneous estimation when highlighting of the homogeneous regions was performed. Figure 11 (a) shows the effect of the current method on dry images. While, Figure 13 (b) shows the result on low contrast images and (c) result on wet fingerprint images, as compared to the existing method.

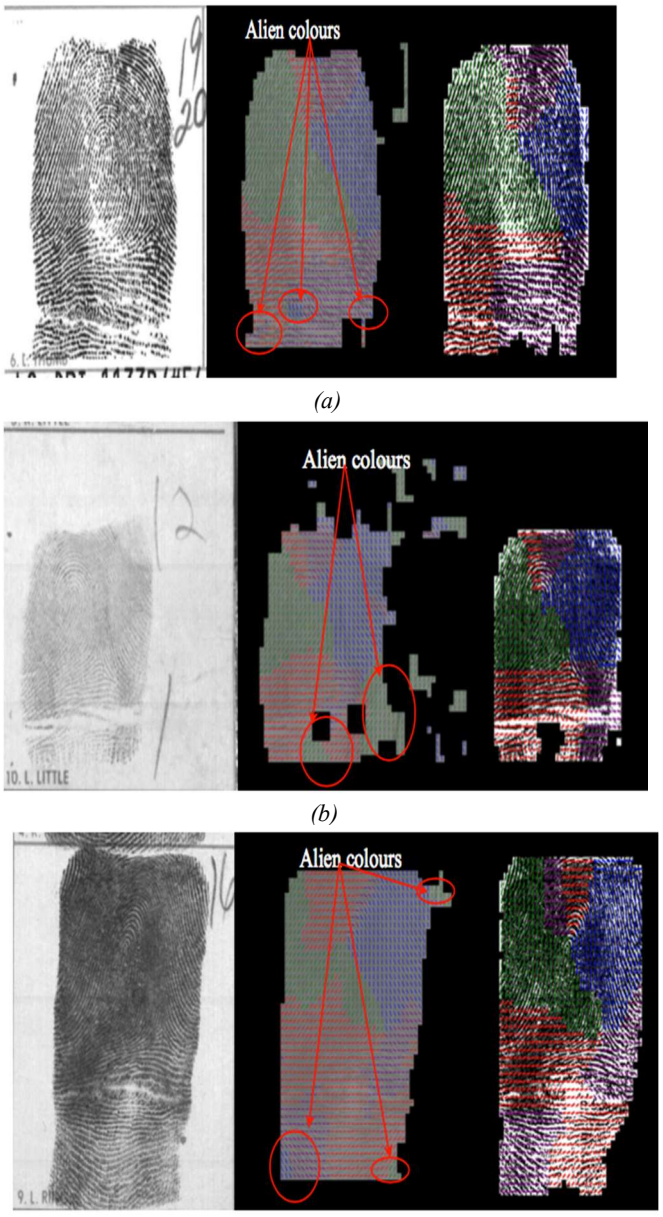

Figure 13: (a), (b), and (c) shows the results of current Orientation fields method on dry, low contrast image and result on wet fingerprint images versus existing method

A goal-directed performance evaluation assesses the overall improvement in the system performance that incorporates the enhancement module as a component.
Therefore, it is capable of providing a more reliable assessment of the performance benchmark and is directly associated with the ultimate goal of the system. In the above results, we present the results of

ISSN: 1992-8645 www.jatit.org E-ISSN: 1817-3195

the goal-directed performance evaluation of our enhancement algorithm.

The global ridge and valley configuration of fingerprint images presents a certain degree of regularity. A global model of the ridges and valleys that can be constructed from partial "valid" regions can be used to correct the errors in the estimated orientation images, which, in turn, will help the enhancement. Currently, we are investigating such a model-based enhancement algorithm. The configurations of ridges and valleys within a local neighborhood vary with the quality of input fingerprint images, therefore some sinusoidal-shaped waves of ridges and valleys may not always be observed. Global features are needed for a more precise region mask classification.

In this paper, it is experimentally demonstrated that the mask used is faster than gradient algorithm in computing orientation field; it performs the computation depending on 8 neighbors of the target block and offers a non-continuous orientation field, resulting in wave pattern links occur during image enhancement filtering. Gradient algorithm can perform the computation in all directions and offer a continuous orientation field. The continuous orientation field and the gradient field allow us to segment any region of the image to blocks of any shape. For image filtering, the precise orientation parameters of gradient algorithm allow us to enhance the fingerprint pattern of different quality images satisfactorily.

5. CONCLUSION

Orientations fields' estimation technique is conveniently and efficiently used to precisely represent the ridge structures. It is noteworthy that, the representation of the ridge structure is challenging because of the limitation in pre-set angles in estimating the orientation fields. This limitation is overcome via newly established Fingerprint Epicycloid filter that utilizes true angles of the orientation fields bearing a resemblance to the natural gradients of fingerprint ridges. Next, a region growing approach is applied for highlighting the homogeneous areas in the fingerprint images. The ultimate outcome of these processes is an image with orientation field representing the actual ridges structure of a fingerprint patterns containing four colours that differentiate each homogenous area in a fingerprint image. The current method was evaluated using different quality images taken from NIST-14 database and outperforms the existing approach in accurate calculations and reliable results on orientation field estimation of fingerprint images.

It is clear that the angular parameters derived from Epicycloid Filter can meet the requirements of actual fingerprint patterns. We can therefore conclude that for orientation field computation, and based on the tested images, the current method is much better than gradient algorithm.

REFERENCES

[1] X. Jiang, "On Orientation and Anisotropy Estimation for Online Fingerprint Authentication," vol. 53, no. 10, pp. 4038–4049, 2005.

[2] D. Maltoni and R. Cappelli, "Advances in fingerprint modeling," *Image Vis. Comput.*, vol. 27, no. 3, pp. 258–268, 2009.

[3] G. Shao, C. Han, T. Guo, and Y. Hao, "An NMF-Based Method for the Fingerprint Orientation Field Estimation," pp. 93–104, 2012.

[4] R. Kumar, P. Chandra, and M. Hanmandlu, "Fingerprint Singular Point Detection Using Orientation Field Reliability," *Adv. Mater. Res.*, vol. 403–408, pp. 4499–4506, Nov. 2011.

[5] D. Informatique, U. Mentouri, R. Ain, and E. Bey, "Ridge frequency estimation for low-quality fingerprint images enhancement using delaunay triangulation," vol. 28, no. 1, 2014.

[6] M. Galar *et al.*, "A survey of fingerprint classification Part I: Taxonomies on feature extraction methods and learning models," *Knowledge-Based Syst.*, vol. 81, pp. 76–97, Jun. 2015.

[7] L. Hong, S. Member, Y. Wan, and A. Jain, "Fingerprint Image Enhancement : Algorithm and Performance Evaluation," vol. 20, no. 8, pp. 777–789, 1998.

[8] A. M. Bazen and S. H. Gerez, "Directional Field Computation for Fingerprints Based on the Principal Component Analysis of Local Gradients," no. November, pp. 1–7, 2000.

[9] E. Zhu, J. Yin, C. Hu, and G. Zhang, "A systematic method for fingerprint ridge orientation estimation and image segmentation," vol. 39, pp. 1452–1472, 2006.

[10] H. Liu, X. Lv, X. Li, and Y. Liu, "Fingerprint Orientation Field Estimation :

ISSN: 1992-8645 www.jatit.org E-ISSN: 1817-3195

Model of Primary Ridge for Global Structure and Model of Secondary Ridge for Correction," pp. 246–255, 2010.

[11] W. Bian, Y. Luo, D. Xu, and Q. Yu, "Fingerprint ridge orientation field reconstruction using the best quadratic approximation by orthogonal polynomials in two discrete variables," *Pattern Recognit.*, vol. 47, no. 10, pp. 3304–3313, Oct. 2014.

[12] Y. Wang, J. Hu, and F. Han, "Enhanced gradient-based algorithm for the estimation of fingerprint orientation fields q," vol. 185, pp. 823–833, 2007.

[13] M. Liu, S. Liu, and Q. Zhao, "Fingerprint orientation field reconstruction by weighted discrete cosine transform," vol. 1, pp. 1–13, 2013.

[14] C. Gottschlich and P. Mih, "Robust Orientation Field Estimation and Extrapolation Using Semilocal Line Sensors," vol. 4, no. 4, pp. 802–811, 2009.

[15] D. M. M. B.G. Sherlock, "A m o d e l for i n t e r p r e t i n g f i n g e r p r i n t t o p o l o g y," vol. 26, no. 7, 1993.

[16] D. Nie, L. Ma, X. Xiao, and S. Xiao, "Optimization Based Fingerprint Direction Field Estimation," pp. 6265–6268, 2005.

[17] J. Li, W. Yau, and H. Wang, "e c d e t p m n a s u," 2007.

[18] P. Gupta and P. Gupta, "Fingerprint Orientation Modeling Using Symmetric Filters," in *2015 IEEE Winter Conference on Applications of Computer Vision*, 2015, pp. 663–669.

[19] Z. Hou, W. Yau, and Y. Wang, "A review on fingerprint orientation estimation," no. June 2010, pp. 591–599, 2011.

[20] X. Liu, M. Pedersen, C. Charrier, F. A. Cheikh, and P. Bours, "An improved 3-step contactless fingerprint image enhancement approach for minutiae detection," in *2016 6th European Workshop on Visual Information Processing (EUVIP)*, 2016, pp. 1–6.

[21] A. Çavuşoğlu and S. Görgünoğlu, "A fast fingerprint image enhancement algorithm using a parabolic mask," *Comput. Electr. Eng.*, vol. 34, no. 3, pp. 250–256, May 2008.

[22] J. Feng, J. Zhou, S. Member, and A. K. Jain, "Orientation Field Estimation for Latent Fingerprint Enhancement," vol. 35, no. 4, pp. 925–940, 2013.